# Structure and thermal stability of MOCVD ZrO2 films on Si (1 0 0)

Wu, X.; Landheer, D.; Graham, M. J.; Chen, H. -W.; Huang, T. -Y.; Chao, T. -S.



**Publisher's version / Version de l'éditeur:**
https://doi.org/10.1016/S0022-0248(03)00827-3
*Journal of Crystal Growth, 250, 3-4, pp. 479-485, 2003-04*

Available online at www.sciencedirect.com
SCIENCE DIRECT®
Journal of Crystal Growth 250 (2003) 479–485
JOURNAL OF CRYSTAL GROWTH
www.elsevier.com/locate/jcrysgro

# Structure and thermal stability of MOCVD $ZrO_2$ films on Si (1 0 0)

X. Wu[a,*], D. Landheer[a], M.J. Graham[a], H.-W. Chen[b], T.-Y. Huang[b], T.-S. Chao[c]

[a] *Institute for Microstructural Sciences, National Research Council of Canada, Ottawa, Ont., Canada K1A 0R6*
[b] *Institute of Electronics Engineering, National Chiao-Tung University, Hsinchu 300, Taiwan*
[c] *Department of Electrophysics, National Chiao-Tung University, Hsinchu 300, Taiwan*

Received 17 October 2002; accepted 23 December 2002
Communicated by D.P. Norton

**Abstract**

The structure and thermal stability of $ZrO_2$ films grown on Si (1 0 0) substrates by metalorganic chemical vapor deposition have been studied by high-resolution transmission electron microscopy, selected area electron diffraction and X-ray energy dispersive spectroscopy. As-deposited films consist of tetragonal $ZrO_2$ nanocrystallites and an amorphous Zr silicate interfacial layer. After annealing at 850°C, some monoclinic phase is formed, and the grain size is increased. Annealing a ~6 nm thick film at 850°C in $O_2$ revealed that the growth of the interfacial layer is at the expense of the $ZrO_2$ layer. In a 3.0 nm thick Zr silicate interfacial layer, there is a 0.9 nm Zr-free $SiO_2$ region right above the Si substrate. These observations suggest that oxygen reacted with the Si substrate to grow $SiO_2$, and $SiO_2$ reacted with $ZrO_2$ to form a Zr silicate interfacial layer during the deposition and annealing. Oxygen diffusion through the tetragonal $ZrO_2$ phase was found to be relatively easier than through the monoclinic phase.


*PACS:* 68.37; 61.14; 77.84; 81.15

*Keywords:* A1. Interfaces; A1. Transmission electron microscopy; A3. Metalorganic chemical vapor deposition; B2. Dielectric materials

## 1. Introduction

There is increasing interest in replacing silicon dioxide with high dielectric constant (high-$\kappa$) materials as gate dielectrics in deep submicron complementary metal-oxide-semiconductor (CMOS) technology [1,2]. In the past few years, extensive study on high-$\kappa$ gate dielectric materials has narrowed down the available choices to some prime candidates such as $HfO_2$, $ZrO_2$ and their silicates. However, the integration of such high-$\kappa$ alternatives into the current CMOS technologies remains a huge challenge mainly due to the stability and interfaces of these high-$\kappa$ dielectrics in contact with the Si substrate [1]. $ZrO_2$ has a high dielectric constant (~25), a high bandgap energy (5.8 eV) and a suitable band offset on Si (1.4 eV) [3]. Although thermodynamic

*Corresponding author. Tel.: +613-9937823; fax: +613-9526337.
*E-mail address:* xiaohua.wu@nrc.ca (X. Wu).

0022-0248/03/$ - see front matter 
doi:10.1016/S0022-0248(03)00827-3

calculations suggest that $ZrO_2$ should not react directly with silicon substrates to form an $SiO_2$ interfacial layer [4], in practice it is difficult to avoid the formation of this low-$\kappa$ interfacial layer during the deposition and post-annealing [5,6].

$ZrO_2$ (as well as $HfO_2$) is known to have three low-pressure structural phases, with monoclinic (m), tetragonal (t), and cubic (c) phases appearing with increasing temperature. The m–t transition takes place near 1100°C, and t–c transition takes place near 2400°C. It has been found that t- and c-$ZrO_2$ are fast ion conductors, while m- $ZrO_2$ is not a fast ion conductor [7,8]. The diffusivities of O in t- and c-$ZrO_2$ are much higher than the diffusivity of O in m-$ZrO_2$ [7]. Annealing $ZrO_2$ in an oxygen-containing atmosphere may be beneficial for the interface structure of the films deficient in oxygen, but t-, c-$ZrO_2$ are excellent ionic conductors. This could result in excess diffusion of oxygen to the interface, ultimately forming an excessively thick $SiO_2$ interfacial layer. From this point of view, obtaining an m-$ZrO_2$ film would have the advantage of limiting interfacial $SiO_2$ layer formation during the post-annealing. Although m-$ZrO_2$ is a room-temperature stable phase, nonequilibrium thermodynamic conditions during deposition result in t-, c-$ZrO_2$ being formed.

There are some controversial results on the interfacial layer between the silicon substrate and the $ZrO_2$ layer. A study of the structure and stability of ultrathin $ZrO_2$ layers on Si(1 0 0) showed that the interfacial layer is pure $SiO_2$, and $ZrO_2$ is remarkably stable against silicate formation up to 900°C, i.e. there is no reaction between $SiO_2$ and $ZrO_2$ [9]. Other studies showed that the interfacial layer is not pure $SiO_2$, but includes Zr atoms [5,6,10]. This Zr-silicate interfacial layer could be formed as the result of the reaction between Si and $ZrO_2$ [10], but could also be formed by the reaction between $SiO_2$ and $ZrO_2$. The latter requires the initial formation of an $SiO_2$ layer by the reaction of Si with oxygen. This paper presents high-resolution transmission electron microscopy (HRTEM), selected area electron diffraction (SAED) and X-ray energy dispersive spectroscopy (XEDS) studies of $ZrO_2$ films grown on Si(1 0 0) by metalorganic chemical vapor deposition (MOCVD). The emphasis is on the structure and thermal stability of the $ZrO_2$ and interfacial layers.

## 2. Experimental procedures

Si (1 0 0) substrates, 100 nm diameter, n-type ($\rho = 0.02-0.06\,\Omega\,cm$) were given an HF-last RCA clean prior to film deposition. The CVD chamber is equipped with a 360l/s turbomolecular pump and a liquid injection system (LDS-300B produced by ATMI). The latter consisted of a liquid pump to pump the precursor, a 0.15 molar solution of $(C_3H_7O)_2(C_{11}H_{19}O_2)_2Zr$ in octane, through a hot glass frit at a rate of 0.2 ml/min. The vapors were carried with a 50 sccm flow of Ar to a gas distribution ring 10 cm from the substrate. The glass frit, the components of the vaporizer, the gas ring and the connecting tube were maintained at a temperature of 190°C with heating tapes and blankets, while the substrate temperature was controlled in the range 390–550°C with quartz-halogen lamps and a thermocouple. The films used in this study were deposited at 390°C. Oxygen was introduced into the chamber at flow rates of 0–150 sccm through a separate gas distribution ring 30 cm from the substrate. Just prior to deposition the wafers were heated for 10 min at 500°C in 10 mTorr of $O_2$ to replace the surface hydrogen termination with oxygen.

The wafers were cut into pieces after deposition and annealed in a Heatpulse 610 (Steag RTP Systems) rapid thermal processing system. For the cross-section TEM sample preparation, two bars were cut out of a wafer, and were glued together with the film sides face-to-face to make the central part of the 3 mm diameter cross-section sample disc. Then the disc was mechanically thinned to $\sim$100 μm thickness. The thinned disc was dimpled from both sides with 3 μm diamond paste until the center of the disc was $\sim$20 μm thick, and then polished from both sides with 1 μm diamond paste to get a very smooth surface. The final thinning until perforation was conducted using Ar ion-

milling from both sides using an ion beam angle of 8°, and a gun voltage of 6 kV. The TEM sample was examined in a Philips EM430 T and a Hitachi HD-2000 scanning transmission electron microscope equipped with a cold field emission gun and an XEDS system.

## 3. Results and discussion

In order to study the $ZrO_2$ film morphology, a 60 nm thick film was grown. Fig. 1a is a cross-section HRTEM image of the film (note that only part of the $ZrO_2$ layer is shown in this figure).

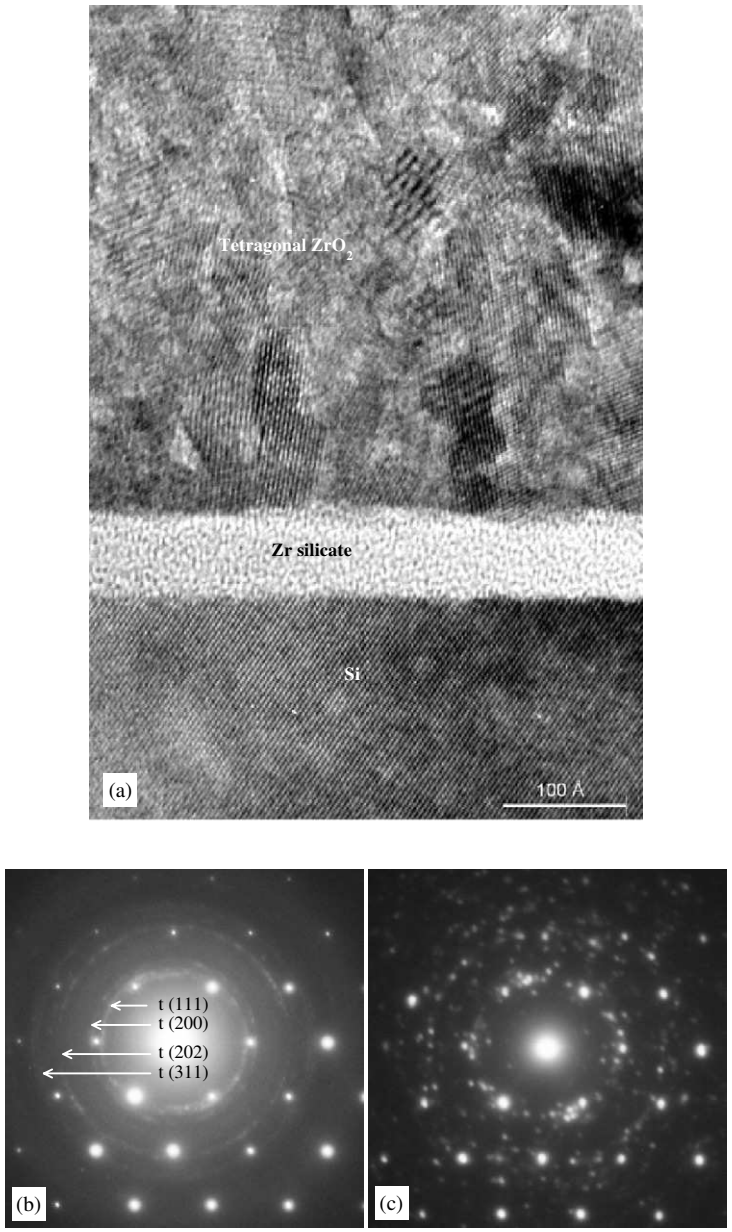


Fig. 1. (a) HRTEM image of an as-deposited $ZrO_2$ film; (b) SAED pattern of the film shown in (a); and (c) SAED pattern of the same film after annealing at 850°C in $N_2$ for 2 min.

Clearly, the $ZrO_2$ film is polycrystalline consisting of many nanocrystallites. There is also a 6.1 nm thick amorphous interfacial layer. Fig. 1b shows a SAED pattern obtained from the film. Diffraction spots are due to the silicon substrate, and the silicon substrate was titled to the [0 1 1] zone axis. This [0 1 1] silicon diffraction pattern is used as a calibration standard to determine the plane spacing of $ZrO_2$. The rings are due to nanocrystalline $ZrO_2$. The relationship between a certain plane spacing ($d$) and the corresponding diffraction pattern (either rings or spots) is given by

$$Rd = \lambda L, \tag{1}$$

where $R$ is either the ring radius or the separation of the direct (center) and diffracted beams as measured on the diffraction pattern, $L$ is the camera length, and $\lambda$ is the wavelength of electrons at the given accelerating voltage. $\lambda L$ is a constant for a certain TEM operation condition. Since we know the spacing ($d$) of plane ($h\,k\,l$) of Si ($d = a/\sqrt{h^2 + k^2 + l^2}$, where $a = 0.5431$ nm, is the lattice constant of Si), the constant $\lambda L$ can be determined using Eq. (1) with the diffraction spots of the silicon. Using a simple data extraction technique called electron diffraction image processing [11], the plane spacings corresponding to the rings were determined as $d_1 = 0.2954$ nm, $d_2 = 0.2544$ nm, $d_3 = 0.1836$ nm and $d_4 = 0.1553$ nm. Comparing the plane spacing data with the tabulated tetragonal $ZrO_2$ plane spacing [12], the rings are indexed completely as tetragonal $ZrO_2$ (t-$ZrO_2$) with the lattice constants $a = 0.512$ nm, $c = 0.525$ nm, and the corresponding planes are indicated in Fig. 1b. The result agrees with the recent study by Perkins et al. [13]. The SAED pattern of an 850°C, 2 min $N_2$ annealed film (Fig. 1c) contains two features of interest. Firstly, the contours of the rings due to tetragonal $ZrO_2$ are still there, but much less continuous compared to the SAED pattern of the as-deposited film (Fig. 1b), which is due to the larger grain size after annealing. Secondly, in addition to the diffraction spots of the Si substrate, there appear many distinct spots unlike any features shown in Fig. 1b. These spots are due to monoclinic $ZrO_2$ with the lattice constants $a = 0.515$ nm, $b = 0.521$ nm, $c = 0.531$ nm, $\alpha = 90°$, $\beta = 99.2°$ and $\gamma = 90°$ [14]. Thus, some metastable tetragonal $ZrO_2$ phase transformed into the stable monoclinic phase, and the film contains mixed tetragonal and monoclinic $ZrO_2$ phases after annealing.

An ultrathin film was grown for further structural analysis. The as-deposited film (Fig. 2a) consists of a 4.6 nm thick, polycrystalline $ZrO_2$ layer and a 1.4 nm thick, amorphous interfacial layer. It is extremely difficult to obtain diffraction patterns from such a thin film by TEM. Instead, we performed fast Fourier transforms on the recorded HRTEM image to obtain the electron diffraction pattern from the $ZrO_2$ layer. These diffraction patterns revealed that the $ZrO_2$ is in the metastable tetragonal phase. The plane spacings of individual grain were also measured directly from the HRTEM. Most of the measured values of plane spacings are between 0.295 and 0.296 nm and this is the (1 1 1) plane placing of tetragonal $ZrO_2$ [12]. X-ray photoelectron spectroscopy (XPS) analysis showed that the interfacial layer is not a pure $SiO_x$, but a Zr silicate layer [5], which is in agreement with a recent study [10].

Two pieces of wafer were annealed in $O_2$ at 850°C. One annealed for 20 s, and the other was annealed for 2 min. Figs. 2b and c are HRTEM images of these two samples. The two annealed samples showed a similar structure to the as-deposited film: a polycrystalline $ZrO_2$ film with an amorphous interfacial layer. The total thickness of the polycrystalline $ZrO_2$ layer and amorphous interfacial layer was 6.2 and 5.9 nm for the two samples, that is essentially unchanged compared with the as-deposited film, 6.0 nm. The thickness of the individual $ZrO_2$ layer and interfacial layer, however, was changed: the interfacial layer thickness increased from 1.4 to 2.7 nm for 20 s annealing, and to 3.7 nm for 2 min annealing, while the $ZrO_2$ layer thickness decreased from 4.6 to 3.4 nm for 20 s annealing and to 2.2 nm for 2 min annealing. The growth of the interfacial layer is at the expense of the $ZrO_2$ layer.

The Zr and O distributions of the annealed film shown in Fig. 2b were determined using XEDS. A line scan was performed from the surface to the substrate to record the O, Zr and Si $K$ edges simultaneously. The scan path is perpendicular to

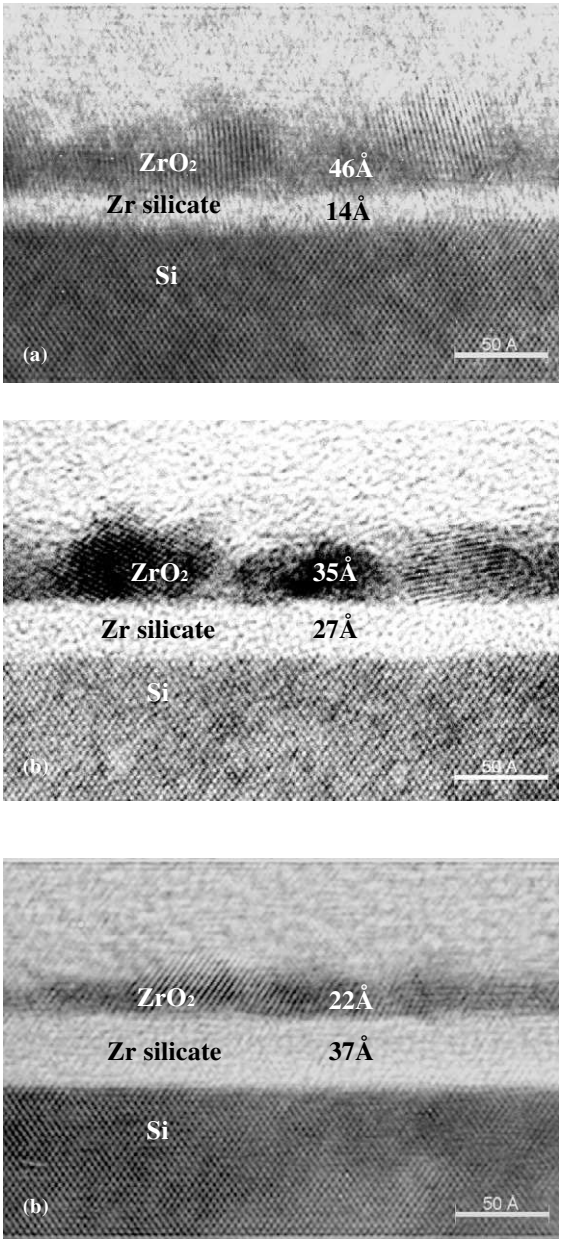


Fig. 2. HRTEM images of a $ZrO_2$ film: (a) as-deposited; (b) annealed at 850°C in $O_2$ for 20 s; and (c) annealed at 850°C in $O_2$ for 2 min.

the interface. The electron probe diameter is 0.5 nm, so the layer thicknesses obtained from XEDS measurement may not be exactly same as by HRTEM. The intensities of the O, Zr and Si $K$ edges are extracted from each point. Fig. 3 shows

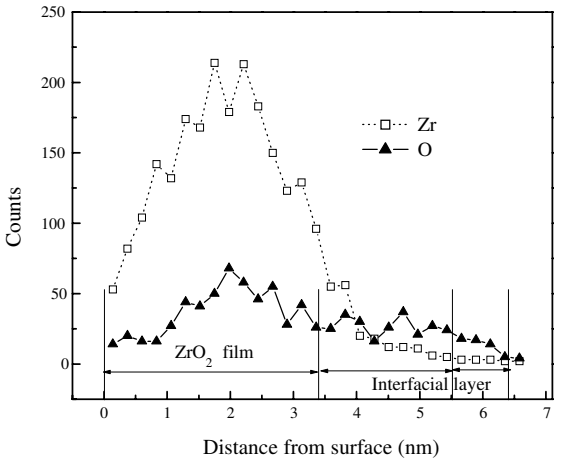


Fig. 3. XEDS profiles of O and Zr of the annealed $ZrO_2$ film shown in Fig. 2b.

the O and Zr profiles. The intensity of each element shown in Fig. 3 has not been corrected to reflect the relative concentrations in the film. In the $ZrO_2$ layer (from 0 to 3.4 nm), both Zr and O counts exhibited an inverse "V" shape distribution, the highest counts being reached around the middle of the film. This type of distribution of Zr and O counts has been reported in a Zr silicate film [15]. The ratio of the counts of Zr to O is not a constant at each position, which means that the composition is not stoichiometric $ZrO_2$ throughout the layer. In the amorphous interfacial layer (from 3.4 to 6.4 nm), Zr was detected and this interfacial layer was revealed by XPS to be a Zr silicate. However, Zr is present only in the upper part (3.4–5.5 nm) of the interfacial layer, and there is no Zr in the lower part (from 5.5 to 6.4 nm). This indicates that there are two distinct layers in the amorphous interfacial layer: a 2.1 nm thick Zr silicate layer and a 0.9 nm thick Zr-free silicon oxide region adjacent to the Si substrate. The presence of this thin pure silicon oxide layer is a significant result. This thin silicon oxide could serve as an "ideal" $SiO_2$-like interface, which is essential for $ZrO_2$ or any other high-$\kappa$ gate dielectric to be integrated into CMOS technology. However, the 0.9 nm thick Zr-free silicon oxide is thicker than an "ideal" interface, and it would compromise the capacitance gain from the high-$\kappa$

$ZrO_2$ layer. The thickness of Zr-free silicon oxide should be controlled during the deposition and annealing treatments, and kept less than 0.5 nm.

The above observations suggest that the most likely mechanism of formation of the Zr silicate interfacial layer on top of the Zr-free silicon dioxide region is that oxygen reacted with the Si substrate to grow $SiO_2$, and $SiO_2$ reacted with $ZrO_2$ to form Zr silicate. During the deposition and annealing treatments, any excess of oxygen will lead to rapid oxygen diffusion through the $ZrO_2$, resulting in $SiO_2$ and Zr silicate formation. In the precursors used for the deposition, $(C_3H_7O)_2(C_{11}H_{19}O_2)_2Zr$, the Zr is co-ordinated to six O atoms, while only two are required to form the $ZrO_2$. This leaves four oxygen atoms per molecule that may release active oxygen during the decomposition of the precursor. Using O-free Zr precursors such as nitrogen co-ordinated precursors, and controlling the post-annealing conditions by using spike anneals and reduced oxygen partial pressure anneals may reduce the interfacial layer thickness.

In order to study the influence of $ZrO_2$ structure on the growth of the interfacial layer thickness, another piece of wafer was annealed first in $N_2$ for 2 min, then in $O_2$ for 20 s (sample A). HRTEM observation revealed that the interfacial layer thickness of this sample is 2.3 nm, slightly less than 2.7 nm of the sample (Fig. 2b) annealed in $O_2$ for 20 s without a prior $N_2$ anneal (sample B). The thickness difference between the two samples can be explained by considering the $ZrO_2$ crystal structures before $O_2$ annealing for both samples. After first annealing in $N_2$, sample A consists of both tetragonal and monoclinic $ZrO_2$ phases, while before $O_2$ annealing, sample B contains only the tetragonal $ZrO_2$ phase. As we discussed earlier, the diffusivities of O in t- and c-$ZrO_2$ are much higher than the diffusivity of O in m-$ZrO_2$ [7]. Therefore, O diffusion through the $ZrO_2$ layer in sample B is relatively easier than in sample A, which results in the thicker interfacial layer in sample B. This observation suggests that before $O_2$ annealing, obtaining m-$ZrO_2$ may help reduce the unwanted interfacial layer thickness. For the 60 nm thick sample film, the grain size was observed to increase after 850°C $N_2$ annealing; sample A may also have a larger grain size than sample B before $O_2$ annealing, which would help reduce the interfacial layer thickness as well. However, the increase in grain size is limited by the film thickness in this case. The interfacial layer thickness difference is not significant in this study due to the ultrathin $ZrO_2$ layer thickness and ultrasmall $ZrO_2$ grain size.

## 4. Conclusions

(1) As-deposited films consist of a tetragonal $ZrO_2$ nanocrystallite layer and an amorphous Zr silicate interfacial layer. Some tetragonal $ZrO_2$ phase transformed to monoclinic after annealing at 850°C, and the grain size became larger.

(2) Annealing a ~6.0 nm thick film revealed that the growth of the interfacial layer is at the expense of the $ZrO_2$ layer. The total thickness of the polycrystalline $ZrO_2$ layer and the amorphous interfacial layer remains unchanged compared with the as-deposited film. A 3.0 nm thick interfacial layer was determined by XEDS as a Zr silicate layer with a 0.9 nm thick Zr-free silicon oxide region adjacent to the Si substrate. These observations suggest that oxygen reacted with the Si substrate to grow $SiO_2$, and $SiO_2$ reacted with $ZrO_2$ to form a Zr silicate interfacial layer during the deposition and annealing.

(3) Comparing the interfacial layer thickness after annealing a ~6.0 nm thick film in $O_2$ with and without prior $N_2$ anneal suggests that O diffusion through the tetragonal $ZrO_2$ phase is relatively easier than through the monoclinic phase.

## Acknowledgements

K. McIlwrath is acknowledged for the XEDS data acquisition, and the authors are grateful to J.W. Fraser, J.R. Phillips, X. Tong and T. Quance for their technical support.

## References

[1] G.D. Wilk, R.M. Wallace, J.M. Anthony, J. Appl. Phys. 89 (2001) 5243.
[2] R.M. Wallace, G. Wilk, Mater. Res. Bull. 27 (2002) 192.
[3] J. Robertson, J. Vac. Sci. Technol. B 18 (2000) 1785.
[4] K.J. Hubbard, D.G. Schlom, J. Mater. Res. 11 (1996) 2757.
[5] H.-W. Chen, T.-Y. Huang, D. Landheer, X. Wu, S. Moisa, G.I. Sproule, T.-S. Chao, J. Electrochem. Soc. 149 (2002) F49.
[6] Y.Z. Yao-Zhi Hu, S.P. Sing-Pin Tay, J. Vac. Sci. Technol. B 19 (2001) 1706.
[7] U. Brossmann, R. Wurschum, U. Sodervall, H.-E. Schaefer, J. Appl. Phys. 85 (1999) 7646.
[8] B.W. Busch, W.H. Schulte, E. Garfunkel, T. Gustafsson, Phys. Rev. B 62 (2000) R13.
[9] M. Copel, M. Gribelyuk, E. Gusev, Appl. Phys. Lett. 76 (2000) 436.
[10] T. Yamaguchi, H. Satake, N. Fukushima, Appl. Phys. Letts. 80 (2002) 1987.
[11] J.P. McCaffrey, E.B. Svedberg, J.R. Phillips, L.D. Madsen, J. Crystal Growth 200 (1999) 498.
[12] Diffraction data, JCPDS file 17–923.
[13] C.M. Perkins, B.B. Triplett, P.C. McIntyre, K.C. Saraswat, E. Shero, Appl. Phys. Letts. 81 (2002) 1417.
[14] Diffraction data, JCPDS file 36–420.
[15] D.A. Muller, G.D. Wilk, Appl. Phys. Lett. 79 (2001) 4195.